International Journal of Nanomaterials and Chemistry

http://dx.doi.org/10.18576/ijnc/040201

Preparation and Characterization of High Stable Silver Nanoclusters in Ambient Condition

Mostafa Farrag[*] *and Haitham M. El-Bery*

Chemistry Department, Faculty of Science, Assiut University, 71516 Assiut, Egypt.

Received: 2 Mar. 2018, Revised: 22 Apr.2018, Accepted: 28 Apr.2018.
Published online: 1 May 2018.

Abstract: This paper describes a new method to prepare organic-soluble silver nanoclusters (AgNCs) protected by thiophenol (TP) (**1**), 4-fluorothiophenol (4-FTP) (**2**) and 4-methylthiophenol (4-MeTP) (**3**) ligands. Those ligands was chosen to investigate the effect of the substituting group attached to the thiophenol moiety from the point of withdrawing group (fluorine atom) and donating group (methyl group) and their effect in the stability of silver clusters. The optical properties of the as synthesized silver nanoclusters exhibited a broad surface plasmon resonance (SPR) peaks at 464 nm, 474 nm and 475 nm for Ag@SPhX (X= H, F, and Me), respectively. All the three types of silver nanoclusters (**1-3**) are highly stable even when being exposed to air as indicated by their absorption spectra. There is almost no change in the intensity of their UV-vis absorption peaks even after 24 hours of air exposure. Therefore, we succeeded in the separation of highly stable silver nanoclusters versus the ambient oxidative condition. The morphology and particles size of the as synthesized nanoclusters were estimated by using transmission electron microscopy (TEM). It was found that, all the three types of silver clusters have a homogenous particle size distribution, with an average particle size of about 2 nm. The average chemical formula and the silver to ligand (Ag/L) ratio were calculated by thermogravimetric analysis (TGA) of the synthesized silver nanoclusters.

Keywords: Monodisperse silver nanoclusters; stability in ambient condition; surface plasmon resonance; HSPhX (X = H, F, Me).

1 Introduction

Noble-metal nanoclusters have had a substantial impact across a wide range of applications, including catalysis [1-3], sensing [4], photochemistry [5-7], biological applications [6], optoelectronics [8], and energy conversion [9] and medicine [10]. Although silver nanoparticles have very desirable physical properties, good relative abundance and low cost, gold nanoparticles have been widely favored due to their proved stability and ease of use. Unlike gold, silver is notorious for its susceptibility to oxidation, which has limited the development of silver-based nanomaterials that could be used in various applications. Despite, two decades of synthetic efforts, silver nanoparticles that have long-term stability remain unrealized.

In our previous work, we succeeded in preparation of some silver nanoclusters protected by three different ligands 2-phenylethanethiol (2-PET), 4-fluorothiophenol (4-FTP) and L-glutathione (GSH) [11]. Ag@2-PET clusters exhibited high stability properties even after exposure to air for 24 hours. In contrast, Ag@SPhF clusters have lost half of their absorbance after 30 min, then the absorbance decreases even further after exposure of the silver clusters solution to air, the same behaviour was found in case of Ag@SG clusters, but the absorbance decreased slowly by time [11].

An interesting cyclic reduction in an oxidative condition (CROC) method reported the preparation of silver nanoclusters in aqueous solutions of water-alcohol; through which a well-defined optical spectrum was obtained [12]. Bakr et al. synthesized a protected silver nanocluster with eight absorption bands [13]. In another study, a 7 kDa silver nanocluster species was reported [14]. However, the exact composition of these silver clusters was not attained in mass spectrometry analysis, although the silver clusters were estimated to be around 25 silver atoms. Overall, the synthesis, isolation, and precise composition determination still remain a big challenge in Ag cluster research. In Nature 2013, Desireddy et al. succeeded in preparation ultrastable and size selected silver clusters M_4Ag_{44}(p-

[*] Corresponding author E-mail: mostafatum@hotmail.com

$MBA)_{30}$, which estimated by electrospray-ionization mass spectrum (ESI-MS) and its structure was determined by single-crystal X-ray diffraction [15]. Monodisperse Ag_7 clusters stabilized by 2,3-dimercaptosuccinic acid (DMSA) ligand was prepared by a wet chemical method [16].

Herein we report a simple synthetic protocol for the production of high stable organic-soluble silver nanoclusters protected by three different ligands thiophenol (TP), 4-fluorothiophenol (4-FTP) and 4-methylthiophenol (4-MeTP). For the sake of characterization, the optical properties of these silver nanoclusters were studied by UV-vis spectroscopy. The composition and particles size of AgNCs were assessed by thermogravimetric analysis (TGA) and transmission electron microscopy (TEM), respectively. The chemical stability of the prepared silver nanoclusters was examined by UV-vis spectroscopy.

2 Experimental

2.1Chemicals

Silver nitrate ($AgNO_3$, 99% metals basis, Aldrich), sodium borohydride (99% metals basis, Aldrich), thiophenol (TP, 99%, Aldrich), 4-fluorothiophenol (4-FTP, 99%, Aldrich) and 4-methylthiophenol (4-MeTP, 98%, Aldrich) were used for synthesizing the ligand protected silver nanoclusters (for the chemical structure of the used ligands see scheme 1). The solvents used were ethanol (HPLC grade, Aldrich), dichloromethane (HPLC grade, 99.9%, Aldrich) and tetrahydrofuran (THF, HPLC grade, 99.9%, Aldrich). All chemicals were used as received. All glassware was thoroughly cleaned with aqua regia (HCl: HNO_3 = 3:1 v/v), rinsed with double distilled water, and then dried in an oven prior to use.

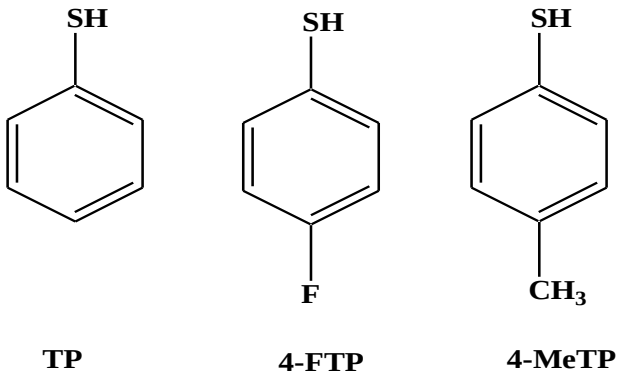

Scheme 1: The ligands used for protecting the synthesized silver nanoclusters, thiophenol (TP), 4-fluorothiophenol (4-FTP), and 4-methylthiophenol (4-MeTP).

2.2 Preparation of Silver Nanoclusters Ag@SPhX (X = H, F, Me)

102 mg of silver nitrate (0.6 mmol) was dissolved in 60 ml absolute ethanol, then the solution was cooled down to around 0°C in an ice bath (30 min). 0.37 ml Thiophenol (TP), 0.38 ml 4-fluorothiophenol (4-FTP) or 0.447 g 4-methylthiophenol (4-MeTP) was added dropwise to the silver solution under stirring speed of 60 rpm. The resulting solution was further stirred in an ice bath at 0°C for 3 hrs under the same stirring speed (60 rpm). The color of silver solution started to change from colerless to bale yellow after the addition of any of the used ligands. Then 22.8 mg of sodium borohydride ($NaBH_4$) was slowly added to the solution under vigorous stirring (~1100 rpm) at 0°C. The solution color turned gradually to deep brown, indicating the reduction of [Ag-ligand] intermediate to silver nanoclusters by $NaBH_4$ (Scheme 2). The reaction was allowed to proceed over night under constant stirring. A brown suspension was finally obtained, and collected through centrifugation (7000 rpm, 10 min) and then washed repeatedly with ethanol to remove the unreacted material. The deep brown solid consisting of Ag@TP, Ag@4-FTP or Ag@4-MeTP nanoclusters was finally dried under reduced pressure in a vacuum desiccators.

3 Results and Discussion

The three types of them as synthesized silver nanoclusters (Ag@TP, Ag@4-FTP and Ag@4-MeTP) were characterized by UV-vis spectroscopy, transmission electron microscopy (TEM), thermogravimetric analysis (TGA), and nitrogen sorption. The stability of the prepared silver nanoclusters was studied in comparison to (Ag@SPhF) silver nanoclusters reported previously [11].

*3.1 Chemical Composition of the Synthesized Silver Nanoclusters (**1-3**)*

The best method to deduce the ratio between organic and metallic part of the protected silver nanoclusters is the thermogravimetric analysis (TGA). With this technique the metal/ligand ratio (M/L) can be derived, thus the average chemical formula of the synthesized silver nanoclusters can be calculated [1,7,17-19].

The three synthesized silver nanoclusters show only one step of mass loss in their thermogravimetric analysis, indicating that the used ligands were decomposed in just one step as presented in (Fig. 1). The weight loss as consequence of the decomposition of the organic ligands; thiophenol (TP), 4-fluorothiophenol (4-FTP) and 4-methylthiophenol (4-MeTP) protected the prepared silver nanoclusters was 30.91 % (wt), 35.96 % (wt) and 34.84 % (wt) (Table 1), respectively. Therefore, the silver content of Ag@TP, Ag@4-FTP and Ag@4-MeTP nanoclusters is

calculated to 69.09 %, 64.04 % and 65.16 % (Table 1), respectively.

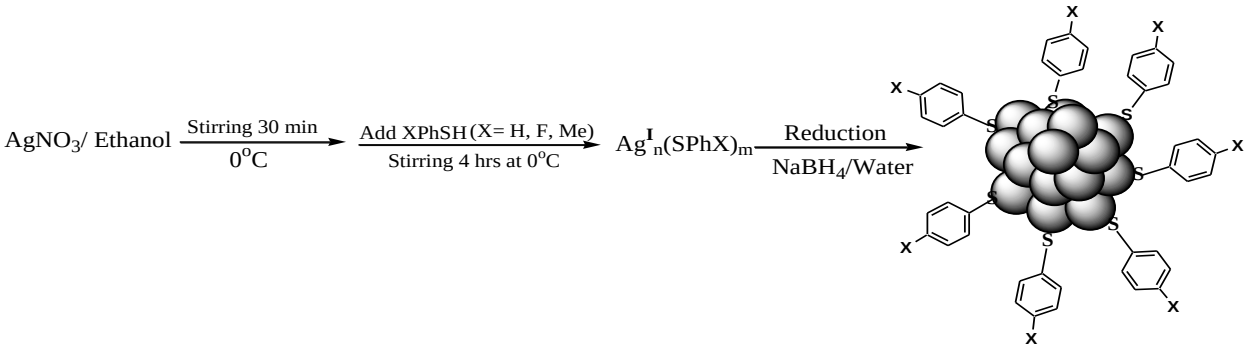

Scheme 2. Preparation steps of Ag@SPhX, (X = H, F, and Me) nanoclusters.

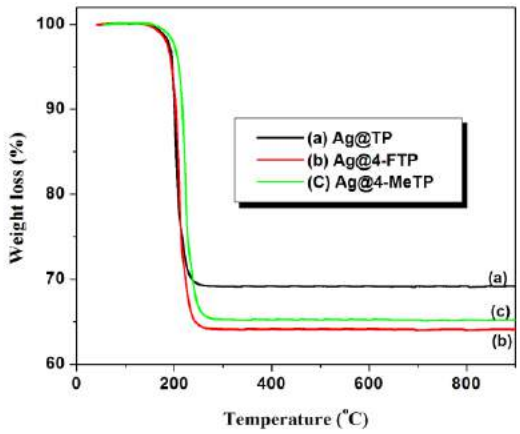

Figure 1: Thermogravimetric analysis (TGA) of Ag@TP (curve a), Ag@4-FTP (curve b) and Ag@4-MeTP (curve c) nanoclusters. Ag@SPhX, (X = H, F, and Me) nanoclusters show one step of mass loss upon heating from 40 to 900°C. The organic part of protected silver nanoclusters (Ag@SPhX) was completely decomposed at around 260 °C, therefore, the residual mass of the clusters samples consists of silver metal atoms only.

From the relative weight of the silver metal residue with respect to the total weight loss of organic ligands, the average metal/ligand (M/L) ratio can be calculated and also the average molecular formula of the synthesized clusters can be derived [1,7,17-19]. The three synthesized silver nanoclusters show nearly the same average molecular formula ($Ag_{2n}L_n$) as shown in Table 1.

*3.2 Particles Size and Morphology of the Synthesized Silver nanoclusters (**1-3**)*

Transmission electron microscopy (TEM) is a powerful technique for determination the average particles size of the metal clusters [1-3,11,17-21], especially if the particle size of synthesized metal nanoclusters is larger than 1 nm, due to the large scattering cross sections of the metal atoms result in a strong contrast in the TEM image. However, if the particles size of protected nanoclusters is less than 1 nm or size selected metal clusters, mass spectrometry should use [19-22]. As in our previous work, we determined the molecular weight of prepared size selected gold clusters (Au_{25}, Au_{38} and Au_{144}) with MALDI-TOF-MS [22].

Fig. 2 (I-III) shows the TEM images of all the three synthesized silver nanoclusters protected by thiophenol (TP), 4-fluorothiophenol (4-FTP) and 4-methylthiophenol (4-MeTP) ligands, respectively. The three synthesized clusters (**1-3**) show individual spherical nanoparticles (Fig. 2). The average particle size of the three silver nanoclusters is around 2 nm. This is a clear indication that, silver nanoclusters with a very narrow size distribution could be obtained with this novel method. Moreover, the average particle size of the synthesized silver nanoclusters was neither affected by withdrawing nor donating groups attached to the thiophenol moiety ligands (Fig. 2).

*3.3UV-Vis Spectra of the Synthesized Silver Nanoclusters (**1-3**)*

Silver and gold nanoparticles within 2-3 nm size have surface plasmon electrons, which appear as surface plasmon resonance peaks in UV-vis spectroscopic analysis [6,11,17,18,23]. These plasmonic metal nanoparticles have a great potential applications in chemical and biological sensor [6,23,24]. In our previous work, silver nanoclusters protected by L-glutathione ($Ag_n(SG)_m$) exhibited two plasmon peaks in the visible region at 478 and 641 nm [6]. These silver clusters (~ 1 nm) show exceptional high biological activity for some bacterial and fungal species [6].

Table 1: Results of the thermogravimetric analysis of the synthesized silver nanoclusters (**1-3**).

No.	Sample	Weight loss (%) (Organic part)	Weight (%) at 900 °C (Metallic part)	M/L* ratio	Molecular formula
1	**Ag@TP**	30.91	69.09	1:0.44	~ $Ag_{2n}L_n$
2	**Ag@4-FTP**	35.96	64.04	1:0.47	~ $Ag_{2n}L_n$
3	**Ag@4-MeTP**	34.84	65.16	1:0.46	~ $Ag_{2n}L_n$

***** M/L means the ratio between the metallic and organic part.

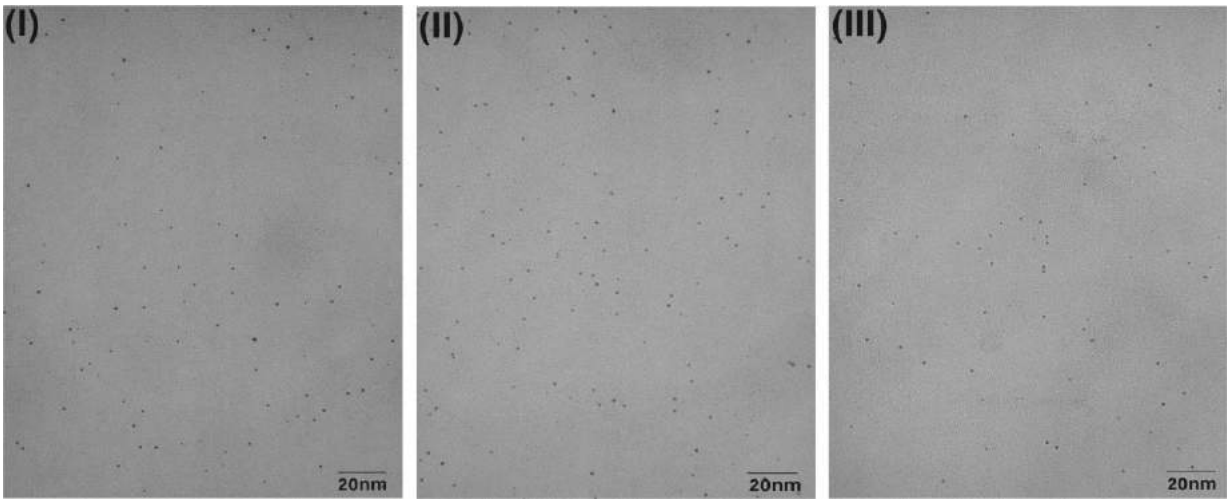

Figure 2: Transmission electron microscopy (TEM) images of silver nanoclusters Ag@SPhX, (X = H, F, and Me), respectively. All the three images look very similar and show clusters of around 2 nm with a very narrow size distribution.

In general silver and gold protected nanoclusters in regime 2 nm exhibit a broad plasmon resonance peaks at around 450 nm and 550 nm, respectively [6,11,17,18]. We have confirmed previously that, for a series from silver nanoclusters in the same size range, the transition can be modeled by Mie theory in combination with the Drude model, which clearly demonstrates that such peaks originate from plasmonic transitions [11].

Fig. 3 shows the spectroscopic analysis of the synthesized silver nanoclusters protected by thiophenol (TP), 4-fluorothiophenol (4-FTP) and 4-methylthiophenol (4-MeTP) ligands. Those silver nanoclusters based on thiophenol moiety, Ag@SPhX (X = H, F, and Me), exhibited a broad surface plasmon resonance (SPR) peaks at 464 nm, 474 nm and 475 nm, respectively (Fig. 3).

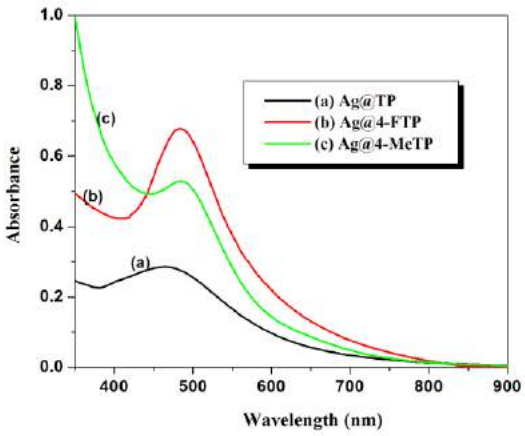

Figure 3: UV−vis absorption spectra of Ag@TP (curve a), Ag@4-FTP (curve b) and Ag@4-MeTP (curve c) nanoclusters. The silver nanoclusters Ag@SPhX, (X = H, F, and Me) exhibit a one intense peak at 464 nm, 474 nm and 475 nm, respectively.

*3.4 Stability of the Synthesized Silver Nanoclusters (**1-3**)*

Noble metal (Pt, Pd, Au and Ag) protected nanoclusters are stable if stored in their solid state phase [1-7,11,15-19]. Moreover, gold, platinum and palladium nanoclusters are also stable if stored in solution (liquid phase) under ambient condition [1-3,7,18-22]. However, the stability of liquid phase protected silver nanoclusters in ambient condition is very poor [11,18,25]. UV-vis spectroscopic analysis was usually used to investigate the stability of protected metal clusters [11,17,18,25]. Whereas, it is sensitive toward metal nanoclusters aggregation and chemical composition changes, which show clear changes in the peak position and/or the intensity of the UV-vis absorbance [11,17,18,25].

For example, in our previous work, the silver nanoclusters protected by 4-fluorothiophenol ligand loosed half of its absorbance after 30 min of air exposure, after that the absorbance decreases quickly with time [11]. A similar behaviour was noticed in case of Ag@SG clusters, its absorbance decreases slowly with time but not as fast as in the previous case [11,18]. Kitaev et al. have synthesized silver nanoclusters in range of 1 nm protected with a mixture of two ligands (captopril and glutathione), using a multistage cyclic reduction in oxidative conditions method [25], these silver clusters lost most of its absorbance within one day exposed to air [25]. Recently, many researchers did the best effort to prepare stable silver nanoclusters in ambient condition [15,17].

The three synthesized silver nanoclusters Ag@SPhX (X = H, F, and Me) exhibited high stability in ambient condition (exposed to air). The synthesized silver nanoclusters are exceptionally stable even when being exposed to air. There was no change in the intensity of the absorption peaks of the UV-vis spectra – a characteristic aging pattern – at all, even after 24 hours under air exposure (Fig. 4). According to this result, the stability of the synthesized silver nanoclusters did not effect by withdrawing group (fluorine atom) or donating group (methyl group) attached to thiophenol ligand moiety. Therefore, with this simple novel synthesis method, we achieved high stable silver nanoclusters under ambient condition.

Fig. 5 shows the kinetic stability study of the synthesized silver nanoclusters (Ag@SPhX) in air, in comparison to the Ag@SPhF clusters (prepared by our old method) [11]. The absorbance percentage of synthesized silver nanocluster (Ag@SPhX) stays completely unchanged over a time period of 24 h. However, Ag@SPhF nanoclusters lost half of its absorbance percentage after 30 min, then its absorbance percentage decreases till less than 20 % after one day exposed to air.

*3.5 Texture Analysis of the Synthesized Silver Nanoclusters (**1-3**)*

The surface and texture properties of the synthesized silver Clusters were studied by sorption of liquid nitrogen at -196 ^{o}C [1-3,7,17]. Gas adsorption/desorption has become one of the most widely used procedures for measuring the surface area and pore size distribution of porous nanomaterials [1-3,7,17].

Liquid nitrogen was used in this work to measure the adsorption–desorption isotherms of the synthesized silver nanoclusters (Fig. 6-I). Fig. 6-I shows the adsorption–desorption isotherms of the three synthesized silver nanoclusters, which are mainly of type II according to Brunaue's classification [1-3,17,26]. According to IUPAC classification of hysteresis loops, the hysteresis loops of all synthesized silver clusters are nearly belonging to type H4 [17,27]. All the three hysteresis loops (Fig. 6-Ia,b,c) are closed at low relative pressure values, which means the synthesized nanoclusters have micropores, as shown in the pore volume distribution curves (Fig. 6-II), which agree with the t-plots analysis (Fig. 6-III). The V_{a-t} plots of all the synthesized silver nanoclusters (Ag@SPhX) exhibited a downward deviation (Fig. 6-III), this confirm the previous suggestion, that these clusters have micropores [28,29]. Table 2 gives the textural data obtained through the analysis of N_2 sorption data of the synthesized silver clusters. The values of surface area which calculated by BET equation (S_{BET}) and t-method (S_t) are close to each other for all investigated clusters (1-3). This confirms the correct choice of standard t-curves for pore analysis and indicates the absence of ultra-micropores in these clusters [29,30]. All clusters (**1-3**) show one maximum sharp peak at ~ 23 Å in pore volume distribution curves (Fig. 6-II). The total pore volume and average pore diameter of all synthesized silver clusters were collected and shown in Table 2.

Table 2: Texture data obtained from the analysis of nitrogen sorption isotherms of the synthesized silver nanoclusters.

No.	Clusters	S_{BET} (m^2g^{-1})	S_t (m^2g^{-1})	Total pore volume (10^{-4}cc g^{-1})	Average pore diameter (Å)
1	**Ag@TP**	6.25	6.25	83.5	90.12
2	**Ag@4-FTP**	6.09	6.10	82.2	90.25
3	**Ag@4-MeTP**	5.99	5.99	82.8	89.83

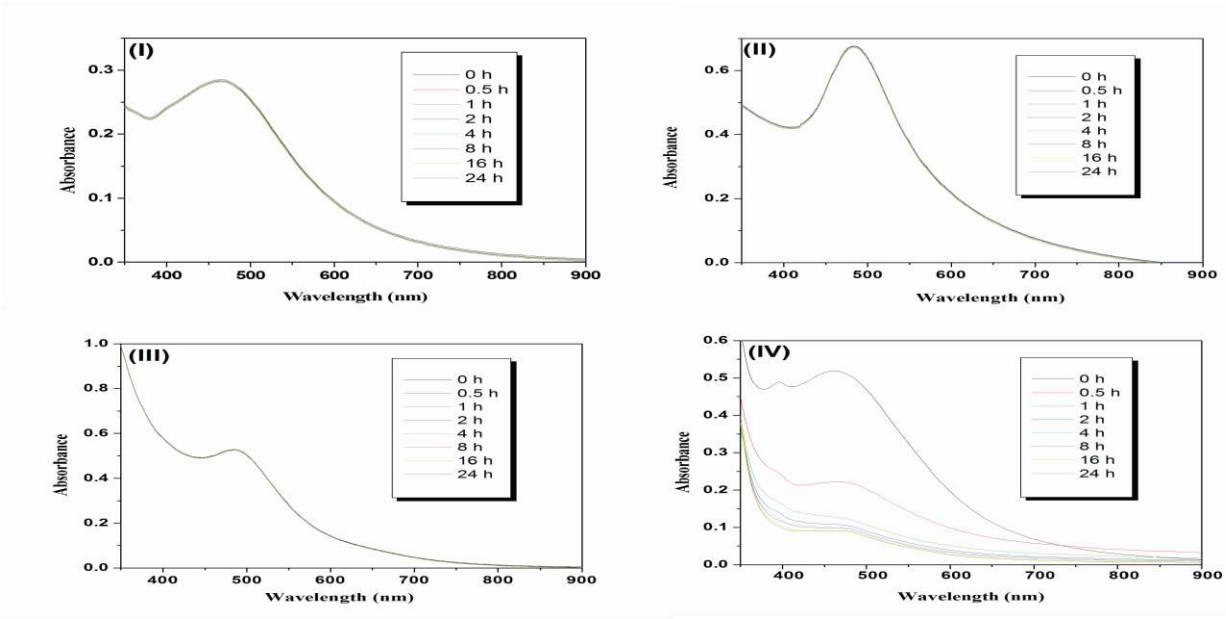

Figure 4: UV-vis absorption spectra of Ag@SPhX nanoclusters as a function of time at ambient condition. The optical spectra of the synthesized silver nanoclusters (Ag@SPhX) stay identical over a time period of 24 hours (**I-III**), respectively. Since UV-vis spectra are rather sensitive to aging, it is concluded that the clusters are stable even under exposure to air. (**IV**) UV-vis absorption spectrum of Ag@SPhF nanoclusters in air (prepared by our old method) [11]. The plasmon peak of the clusters strongly decreases while they are stored in air. Already after 30 minutes the intensity of the peak halved in value. Therefore, it is concluded that these clusters are very sensitive to oxygen. Reprinted with permission from ref. 11. Copyright (2012) American Chemical Society.

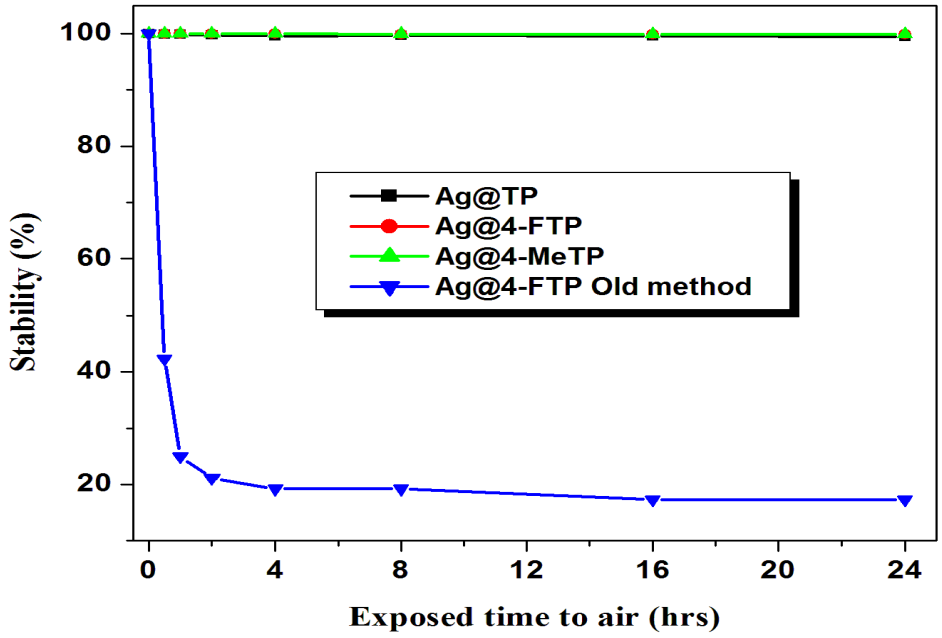

Figure 5: The kinetic study of the stability of synthesized silver nanoclusters (Ag@SPhX) in air. The absorbance percentage of synthesized silver nanocluster (Ag@SPhX) stays completely the same over a time period of 24 h. However, Ag@SPhF nanoclusters (prepared by our old method) [11] loses half of its absorbance percentage after 30 min, then its absorbance percentage decreases till less than 20 % after one day exposed to air.

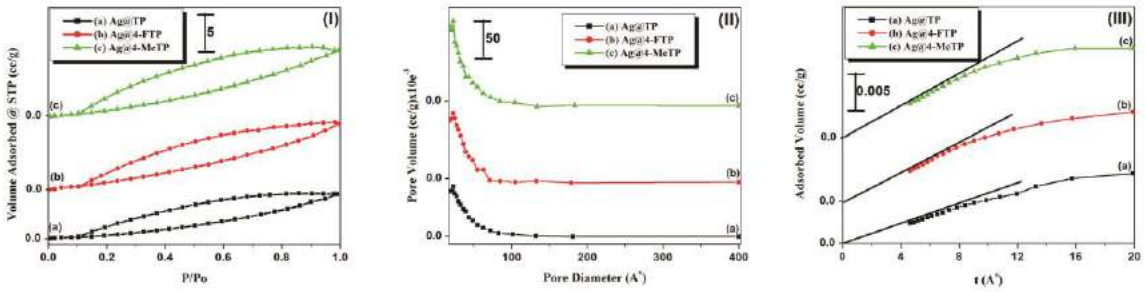

Figure 6 (**I**) Nitrogen adsorption-desorption isotherms (**a-c**) of all synthesized silver nanoclusters protected by thiophenol (TP), 4-fluorothiophenol (4-FTP) and 4-methylthiophenol (4-MeTP) ligands, respectively. All the three isotherms show mainly type II of Brunaue's classification and type H4 hysteresis loops according to IUPAC classification of hysteresis loops. The pore volume distribution curves (**II**) and $V_{a\text{-}t}$ plots (**III**) of all silver nanoclusters (**1-3**). All the three $V_{a\text{-}t}$ plots were exhibited a downward deviation and the three pores volume distribution curves show one maximum sharp peak at ~23 Å, which confirms the protected clusters have micro porous.

4 Conclusions

Herein we report a new synthesis method to prepare highly stable silver nanoclusters under oxidative ambient condition via protecting them by different ligands like thiophenol (TP) (**1**), 4-fluorothiophenol (4-FTP) (**2**) and 4-methylthiophenol (4-MeTP) (**3**). The stability of the synthesized silver nanoclusters did not effect by the attached group to the thiophene moiety, if it is a withdrawing group (fluorine atom) or donating group (methyl group). The used method in this work produces very narrow size distribution silver nanoclusters in the range of 2 nm. The optical properties of the synthesized silver clusters were studied by UV–vis spectroscopy. The synthesized silver nanoclusters Ag@SPhX (X = H, F, and Me) exhibited a broad surface plasmon resonance (SPR) peaks located at 464 nm, 474 nm and 475 nm, respectively. The synthesized silver nanoclusters show high stability in ambient condition, at least after 24 hours exposure to air. The metal-to-ligand ratio (M/L) and the average chemical formula of the prepared silver clusters were calculated from thermogravimetric analysis (TGA). The average M/L ratio of the synthesized silver nanoclusters was around 1/0.45 and the average molecular formula was $Ag_{2n}L_n$. The complete isotherms of the synthesized silver clusters were measured using nitrogen adsorption-desorption process at -196^{o}C, specific surface area S_{BET}, pore volume and average pore diameter were calculated. The hysteresis loops of all synthesized silver nanoclusters belong to type H4. The specific surface areas for the synthesized silver nanoclusters were around 6 m^2/g and their pore volume distribution curves show maximum sharp peak at ~ 23 Å for the three synthesized nanoclusters (**1–3**).

Acknowledgements

This work is supported by Assiut University, Egypt.

References

[1] M. Farrag, J. Mol. Catal. A Chem., 413, 2016, 67.
[2] M. Farrag, Micropor. Mesopor. Mat., 232, 2016, 248
[3] M. Farrag, Micropor. Mesopor. Mat., 257, 2018, 110.
[4] J. N. Anker, W. P. Hall, O. Lyandres, N. C. Shah, J. Zhao and R. P. Van Duyne, Nature Mater., 7, 2008, 442.
[5] R. Jin, Y. C. Cao, E. Hao, G. S. Métraux, G. C. Schatz and C. A. Mirkin, Nature, 425, 2003, 487.
[6] M. Farrag and R. A. Mohamed, J. Photochem. Photobiol. A Chem., 330, 2016, 117.
[7] M. Farrag, J. Photochem. Photobiol. A Chem., 318, 2016, 42.
[8] M. A. Noginov, G. Zhu, A. M. Belgrave, R. Bakker, V. M. Shalaev, E. E. Narimanov, S. Stout, E. Herz, T. Suteewong and U. Wiesner, Nature, 460, 2009, 1110.
[9] H. A. Atwater and A. Polman, Nature Mater., 9, 2010, 205.
[10] R. R. Arvizo, S. Bhattacharyya , R. A. Kudgus , K. Giri , R. Bhattacharya and P. Mukherjee Chem. Soc. Rev., 41, 2012, 2943.
[11] M. Farrag, M. Thämer, M. Tschurl, T. Bürgi and U. Heiz, J. Phys. Chem. C, 116, 2012, 8034.
[12] N. Cathcart, P. Mistry, C. Makra, B. Pietrobon, N. Coombs, M. Jelokhani-Niaraki and V. Kitaev, Langmuir, 25, 2009, 5840.
[13] O. M. Bakr, V. Amendola, C. M. Aikens, W. Wenselers, R. Li, L. D. Negro, G. C. Schatz and F. Stellacci, Angew. Chem., Int. Ed., 48, 2009, 1.
[14] K. V. Mrudula, T. U. B. Rao and T. Pradeep, J. Mater. Chem., 19, 2009, 4335.
[15] A. Desireddy1, B. E. Conn1, J. Guo1, B. Yoon, R. N. Barnett, B. M. Monahan1, K. Kirschbaum, W. P. Griffith, R. L. Whetten, U. Landman and T. P. Bigioni, Nature., 501, 2013,399.
[16] Z. Wu, E. Lanni, W. Chen, M. E. Bier, D. Ly and R. Jin, J.

Am. Chem. Soc., 131, 2009, 16672.
[17] M. Farrag, Mater. Chem. and Phys., 180, 2016, 349.
[18] M. Farrag, M. Tschurl and U. Heiz, Chem. Mater., 25, 2013, 862.
[19] H. Qian and R. Jin, Nano Lett., 9, 2009, 4083.
[20] Y. Shichibu, Y. Negishi, T. Tsukuda and T. Teranishi, J. Am. Chem. Soc., 127, 2005, 13464.
[21] Y. Negishi, N. K. Chaki, Y. Shichibu, R. L. Whetten and T. Tsukuda, J. Am. Chem. Soc., 129, 2007, 11322.
[22] M. Farrag, M. Tschurl, A. Dass and U. Heiz, Phys. Chem. Chem. Phys., 15, 2013, 12539.
[23] P. K. Jain, K. S. Lee, I. H. El-Sayed and M. A. El-Sayed, J. Phys. Chem. B, 110, 2006, 7238.
[24] S. Kumar, M. D. Bolan and T. P. Bigioni, J. Am. Chem. Soc., 132, 2010, 13141.
[25] N. Cathcart and V. Kitaev, J. Phys. Chem. C, 114, 2010, 16010.
[26] S.L. Brunauer, L. S. Deming, W. S. Deming and E. Teller, J. Am. Chem. Soc., 62, 1940, 1723.
[27] IUPAC recommendations for the characterization of porous solids, Pure Appl. Chem., 66, 1994, 1739.
[28] G. Leofanti, M. Padovan, G. Tozzola and B. Venturelli, Catalysis Today, 41, 1998, 207.
[29] M.Th. Makhlouf, B. M. Abu-Zied and T.H. Mansoure, applied surface Science, 274, 2013, 45.
[30] W.M. Shaheen, A.A. Zahran and G.A. El-Shobaky, colloids and surfaces A: physicochemical and engineering aspects, 231, 2003, 51.